

## ELASTOPLASTIC MODELLING OF A FOUNDATION ON AN UNSATURATED SOIL

NUBIA A. GONZÁLEZ\* AND ANTONIO GENS†

\* REPSOL, Madrid, Spain  
e-mail: Nubia.Aurora.Gonzalez@upc.edu

† Departamento de Ingeniería del Terreno  
Universitat Politècnica de Catalunya  
Jordi Girona 1-3, Edificio D2, 08034 Barcelona, Spain  
email: Antonio.gens@upc.edu

**Key words:** Computational Plasticity, Unsaturated Soils, Shallow Foundations

**Abstract.** This paper presents a coupled flow-deformation finite element analysis of a shallow foundation on an unsaturated loosely compacted silt subjected to variations in the water level. The behaviour of the silt foundation was simulated using the Barcelona Basic Model (BBM) which was implemented into the PLAXIS finite element code. Material parameters were calibrated from laboratory tests reported in the literature. The influence of partial soil saturation and of fluctuations of the groundwater level on the behaviour of footing is investigated.

### 1 INTRODUCTION

A common engineering problem which often involves unsaturated soils is that of shallow foundation that rests above the ground water table. In many cases a capillary zone exists above the groundwater level (G.W.L), where the soil is unsaturated. Typical footing analyses ignore this zone and assume that the soil above the ground water table is dry. This type of analyses underestimates the soil strength but, more importantly, ignores well known features of unsaturated soils such as collapse upon wetting.

This paper presents a series of unsaturated finite element analysis of a strip footing on an unsaturated loosely compacted silt performed with PLAXIS program using a fully coupled flow-deformation analysis [1]. Soil behaviour is described using the well-known BBM [2]. The influence of partial soil saturation and of fluctuations of the G.W.L. on the behaviour of footing is investigated.

### 2 CONSTITUTIVE RELATIONS

The main features of the model used herein are: i) to use the BBM formulation and ii) to adopt Bishop stress and suction as the constitutive stress variables,

$$\sigma'_{ij} = \sigma_{ij} - P_a \delta_{ij} + S_e (P_a - P_w) \delta_{ij} \quad (1)$$

$$s = P_a - P_w \quad (2)$$

where,  $\sigma_{ij}$  is the total stress vector,  $P_a$  the air pressure,  $P_w$  the water pressure,  $S_e$  the effective degree of saturation and  $\delta_{ij}$  the Kroneckers's delta. It is assumed that that  $P_a$  is constant and equal to atmospheric; therefore, suction is negative of pore pressure [1].

Hydraulic hysteresis effects are not considered in the formulation. van Genuchten equation is adapted for the description of the relationship between degree of saturation and suction,

$$S_e = \frac{S_r - S_{res}}{S_{sat} - S_{res}} = \left[ 1 + \left( g_a \frac{P_w}{\gamma_w} \right)^{g_n} \right]^{g_c} \quad (3)$$

where,  $S_e$  is the effective degree of saturation,  $S_r$  the degree of saturation,  $S_{res}$  the residual saturation at very high value of suction,  $S_{sat}$  the saturation of saturated soil and  $g_a$  [ $m^{-1}$ ],  $g_n$  and  $g_c$  are fitting parameters,  $g_c$  is often used as  $(1/g_n-1)$ .

The permeability for unsaturated states is computed as

$$k_i = k_{rel} k_i^{sat} \quad i = x, y, z \quad (4)$$

where  $k_{sat}^i$  is the permeability for saturated soils and  $k_{rel}$  is the relative permeability defined by,

$$k_{rel} = (S_e)^{g_l} \left[ 1 - \left( 1 - S_e \left( \frac{-1}{g_c} \right) \right)^{(-g_c)} \right]^2 \quad (5)$$

where,  $g_l$  is a fitting parameter.

Full details of the constitutive model are given in [3,4] and details of the fully coupled flow deformation analysis are given in [1].

### 3 MODEL CALIBRATION

A set of oedometer and triaxial laboratory tests on an unsaturated compacted silty soil (Jossigny silt) reported in [5] has been selected for the calibration of the constitutive model and the shallow foundation analysis performed in this work. Jossigny silt is a low plasticity silt ( $w_P=19$ ,  $w_L=37$ ,  $I_P=18$ ), the normal Proctor optimum characteristics are  $\gamma_{opt}=16kN/m^3$  and  $w_{opt}=18\%$ . It was compacted at low values of dry density and water content ( $\gamma_{dry}=14.5kN/m^3$  and  $w=13\%$ ) to ensure significantly susceptibility to wetting.

The soil water retention curve (SWRC) obtained experimentally by different techniques and the calibrated curve are plotted in Figure 1. The experimental results showed the existence of hysteresis in the SWRC, however, the calibrated curve employed in this work is representative of the wetting branch.

Predicted and experimental results of oedometer tests performed under saturated conditions ( $s=0$  kPa) and at constant suctions of 100 and 200 kPa are plotted in Figure 2, a good agreement between predicted and experimental behavior is observed. Figure 2 also shows the results of a wetting test (starting from  $s=200$  kPa) under a vertical stress of 200 kPa for which it is evident the reduction in volume induced by saturation (collapse behavior).

Predicted and experimental results of a triaxial test involving anisotropic loading prior to shearing at constant suction of 200 kPa are plotted in Figure 3. Predicted behaviour also shows a reasonably good agreement with experiments.

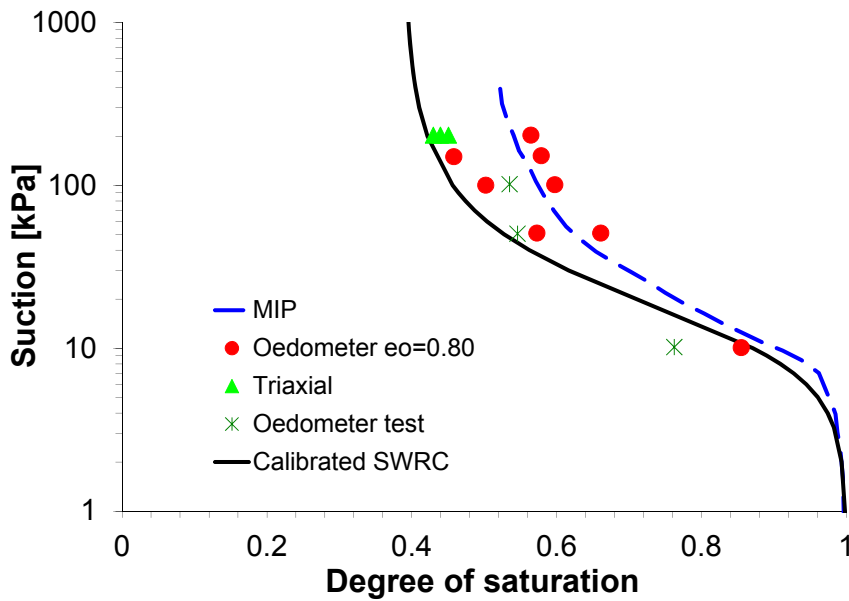


Figure 1: Soil Water Retention Curve of Jossigny silt (Experimental data from [5])

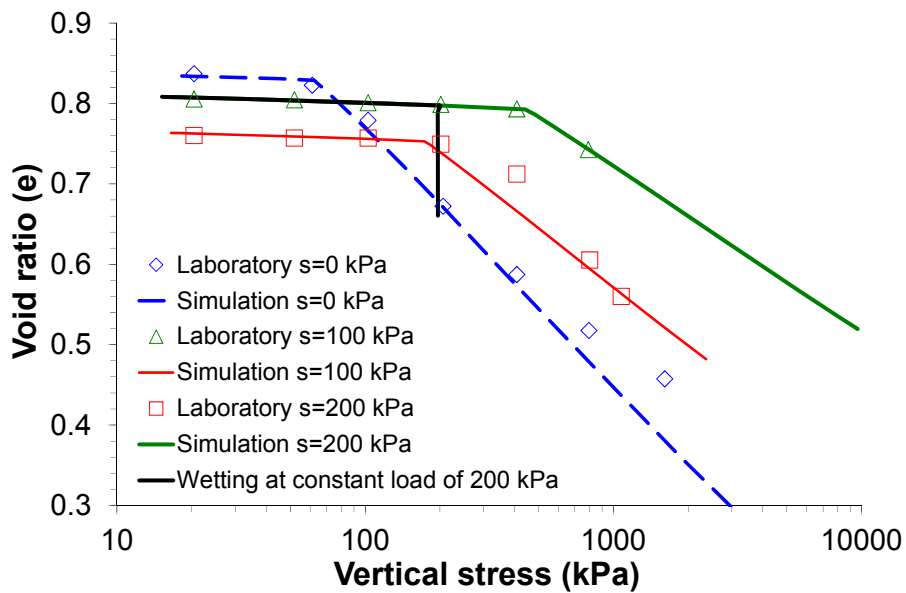
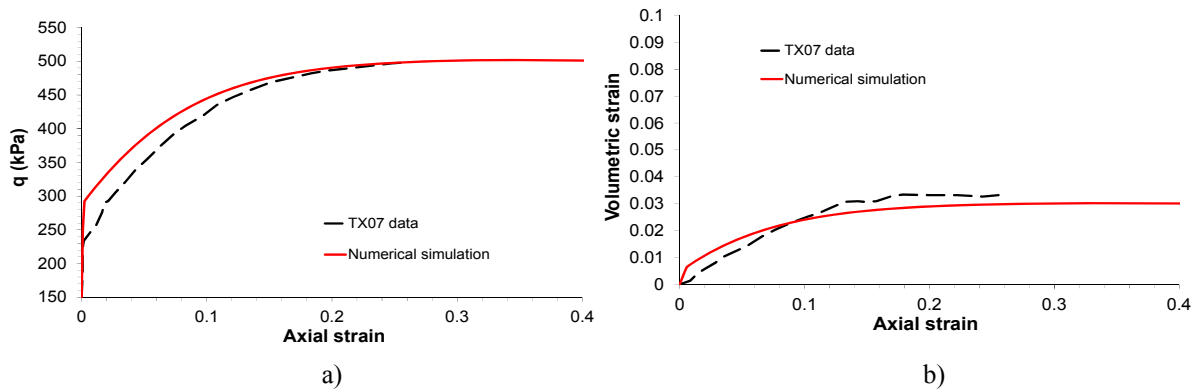


Figure 2: Predicted and experimental behavior of oedometer tests on Jossigny silt (Experimental data from [5])

#### 4 SHALLOW FOUNDATION ANALYSIS

In this section numerical simulation of a smooth strip footing, resting on the compacted Jossigny silt is presented. The mesh consists of 415 15-noded triangular elements with a fourth order interpolation for displacements and for pore pressure and 12 gauss points for each element. The width and height of the model are 10 m and the width of the footing is 1 m. The initial position of the G.W.L. is on the surface. This level is changed during drying and wetting processes. The top, left and right boundaries are closed for flow, and drying and

wetting are only applied through the bottom boundary by linearly changing the water head with time. The yield surface locations for the fully saturated conditions were set considering a preoverburden pressure (POP) of 55 kPa at the ground surface, where POP is defined as the difference between the vertical effective stress and the vertical preconsolidation pressure.



**Figure 3:** Predicted and experimental behavior of a triaxial test on Jossigny silt (Experimental data from [5]). (a) Deviatoric stress ( $q$ ) against axial strain; (b) Volumetric strain against axial strain

Two set of analysis were considered. In the first analysis, the footing was loaded considering three different depths of the G.W.L.: *a*) a deep water level (10 m depth), *b*) a water level at 5 m depth and *c*) a water level at the ground surface (saturated condition). In the second analysis the footing was loaded to a certain load with the G.W.L. at 5 m depth and subsequently the G.W.L. was raised to the ground surface at constant applied load. Three different loads were considered: 75 kPa, 100 kPa and 125 kPa.

#### 4.1 Rigid footing at different groundwater levels

To simulate the behavior of a rigid foundation, the analysis is performed under displacement control with vertical displacements applied to the soil surface below the position of the footing and an equivalent pressure is computed by summing the appropriate vertical nodal reactions. Before applying these displacements, the initial position of the G.W.L. was varied in order to set different initial suction profiles. Three initial positions were analyzed: 0 m, 5 m and 10 m, corresponding to suction values of 0 kPa, 50 kPa and 100 kPa on the top boundary, with the first value corresponding to a fully saturated condition. After the drying phase, the footing was loaded to a total displacement of 0.2 m. This displacement was applied over a time period of 1000 days, so that the rate of loading was slow enough to ensure fully drained conditions.

The predicted load-displacement curves for the three different initial positions of the G.W.L. are shown in Figure 4. The figure shows an increase of the predicted footing load with the G.W.L. depth. The footing load has not reached its limiting value at the maximum displacement achieved in the analysis. The load-displacement behavior is largely controlled by the increase of the elastic domain as illustrated in Figure 5, which plots the stress path followed for a stress point located directly underneath the footing.

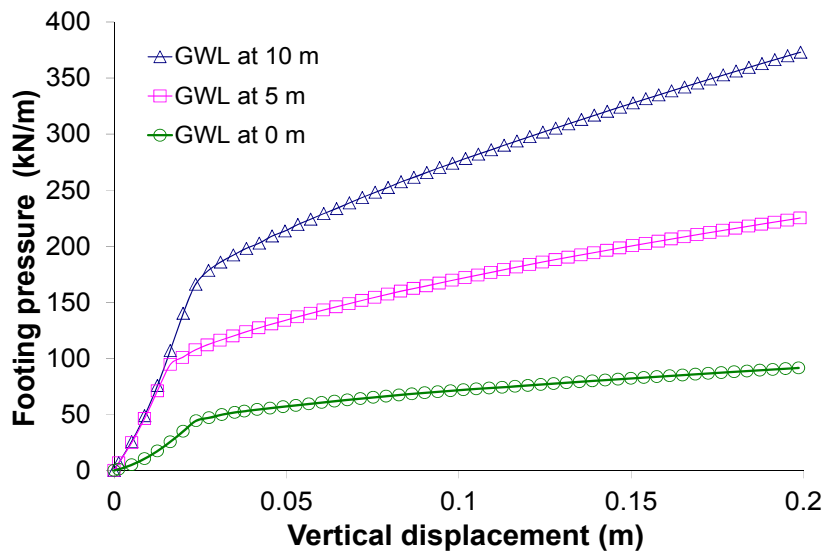


Figure 4: Load-settlement curves of rigid footing with different groundwater levels

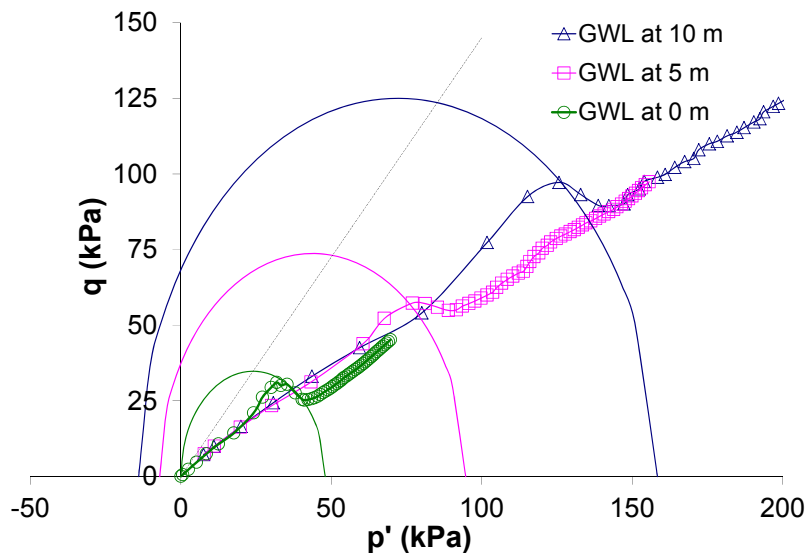


Figure 5: Stress-paths followed by footing for a point located directly underneath the foundation

#### 4.2 Flexible footing with rise of groundwater level

This analysis considers that the strip footing is vertically loaded to three different loads: 75, 100 and 125 kPa with the initial water level at 5.0 m. Then, the surface soil adjacent to the footing is wetted to zero suction (G.W.L. at the ground surface). These boundary conditions were imposed over a time of 1000 days in order to maintain fully drained conditions. As the footing is loaded by a uniform vertical pressure, and not by uniform imposed vertical displacements, it is taken to be perfectly flexible.

Figure 6 shows the relationships between vertical displacements against vertical effective stresses predicted by the three different loads. In the same figure the stress-displacement

curves for G.W.L. at 5.0 m and G.W.L. at 0 m (presented in the previous section) are also plotted for comparison. It can be seen in this figure that the higher the load at which wetting took place the larger the induced settlement. In fact, there is an important reduction in displacement (or swelling behavior) rather than significant settlements when the wetting path is carried out at a load of 75 kPa, while, the wetting paths at loads of 100 kPa and 125 kPa initially exhibited only a small decrease in displacement (swelling), followed by larger settlements (or collapse behavior).

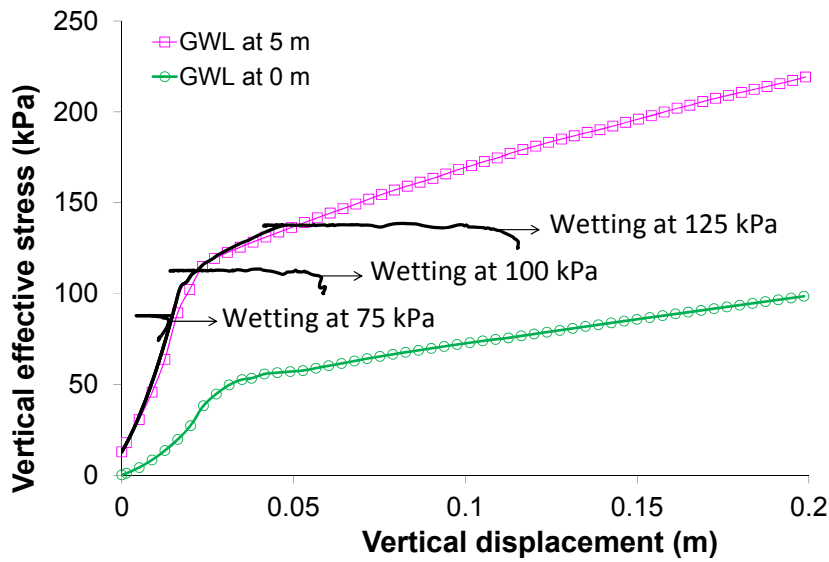


**Figure 6:** Vertical stress-displacement curves for unsaturated wetting analysis

This behavior is controlled depending on the location of the stress state with respect to the yield surface, as is illustrated in Figure 7, which plots the stress paths in the mean Bishop's stress against suction plane. Initial position of the Loading-Collapse (LC) curves just before wetting is also plotted in the figure. It is observed that in the three cases, the wetting paths first occur in the elastic domain until the LC curves are crossed, where, larger irreversible displacements are predicted. However, it is observed that most of the wetting path at a constant load of 75 kPa lies in the elastic domain and therefore a significant elastic swelling is predicted.

The vectors of total displacements after load to 125 kPa and after wetting at constant load of 125 kPa are presented in Figure 8. The orientation of these vectors indicates the direction of movement and their length the relative magnitude of movement (scaled by 40). Wetting of the soil leads to significantly increase of displacements of the nodes below the footing while the nodes away the footing heave.

The displacement pattern for the three analyses is better represented in Figure 9, where the computed vertical displacements after load and after wetting along a cross section at the ground surface are plotted. Negative displacements indicate settlements whereas positive displacements indicate heave of the ground surface. Since the footing is flexible, loading at constant G.W.L. of 5.0 m it causes differential movements with the maximum settlements at its

center ( $x=0$ ), a reduced settlements at the footing edge ( $x=1\text{m}$ ) and an almost zero settlements at the distance of 10 m from its center.

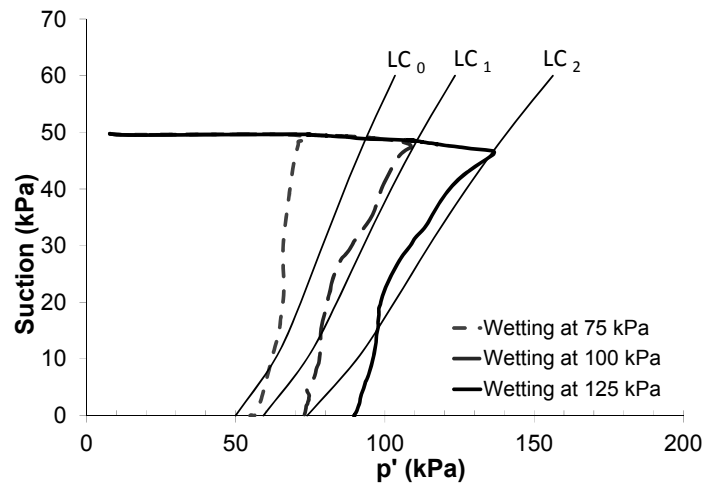


**Figure 7:** Stress paths for the wetting analysis in a point located directly underneath the foundation.  $LC_0$ : initial position of LC curve;  $LC_1$ : LC position after load to 100 kPa;  $LC_2$ : LC position after load to 125 kPa

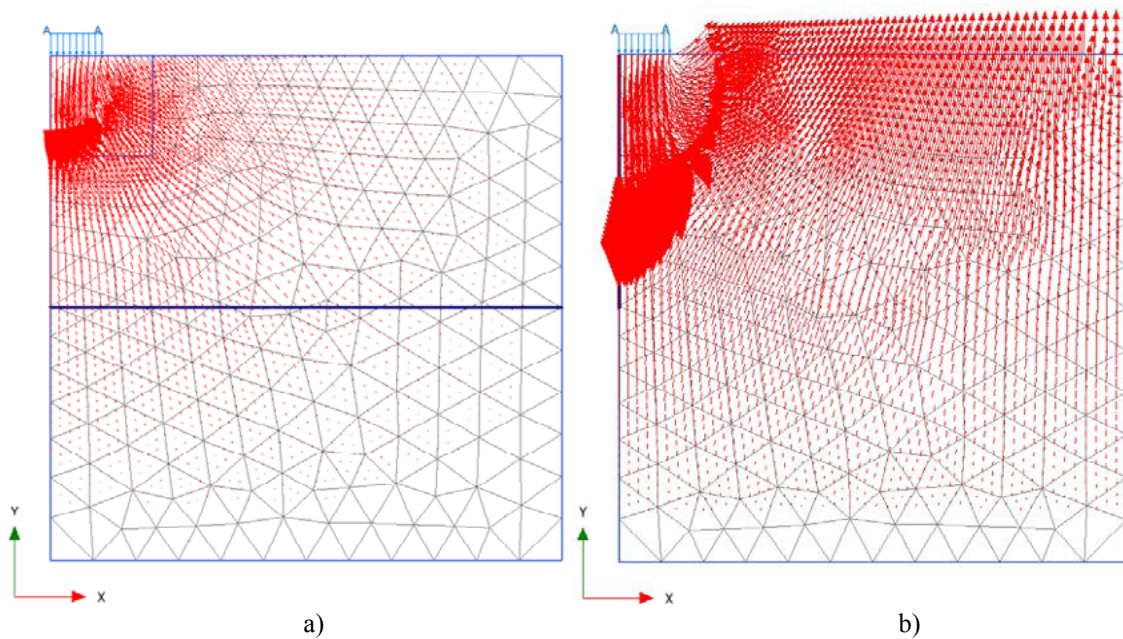


**Figure 8:** Vectors of total displacements. (a) After load to 125 kPa; (b) after wetting to the ground surface

During wetting phase, the ground surface heaves or continues to settle, depending on the distance from the footing center and on the applied load before wetting. At the centre of the footing a further settlement is predicted when the applied loads before wetting are of 100 kPa and 125 kPa, it is not the case when the applied load is of 75 kPa, which causes a settlement reduction. Just underneath the edge of the footing (at  $x=1\text{m}$ ), the vertical displacements after wetting begin to change rapidly from settlement to heave. At distances higher than about 1.25

m away from the footing center, the ground surface rises. Due to the fact that the Jossigny silt has a low swelling index ( $\kappa$ ) of only 0.005 (see Table 1) heave is relatively small.

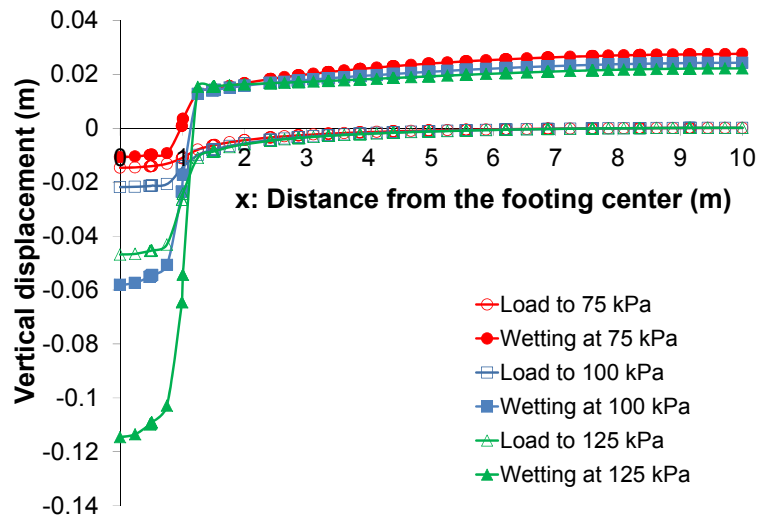


**Figure 9:** Vertical displacements at the ground surface induced by loading and wetting at three different loads

## 5 CONCLUDING REMARKS

The influence of partial soil saturation on the behaviour of a strip shallow foundation lying on a compacted silty soil was investigated through a series of FE analysis. Predicted ultimate footing load increases for larger depths of the G.W.L. Collapse of the foundation was computed when the G.W.L. rises to the ground surface, the higher the applied load before wetting the higher the settlements.

## ACKNOWLEDGEMENTS

The support by the Ministry of Science and Innovation of Spain through grant BIA2011-27217 is gratefully acknowledged.

## REFERENCES

- [1] Galavi, V. *Groundwater flow, fully coupled flow deformation and undrained analysis in PLAXIS 2D and 3D*. Technical internal report, Plaxis BV (2010).
- [2] Alonso E, Gens A. and Josa A. A constitutive model for partially saturated soils. *Géotechnique* (1990) **40**: 405-430.
- [3] González, N.A. and Gens, A. Evaluation of a constitutive model for unsaturated soils: stress variables and numerical implementation. *Fifth International Conference on Unsaturated Soils* (E. Alonso, A. Gens, eds.) **2**: 829-835 (2010).
- [4] González, N.A. *Development of a family of constitutive models for geotechnical applications*. PhD Thesis, Technical University of Catalunya, UPC-BarcelonaTech (2011).
- [5] Casini F. *Effetti del grado di saturazione sul comportamento meccanico di un limo*. PhD Thesis, Sapienza Università di Roma, Italy (2008).